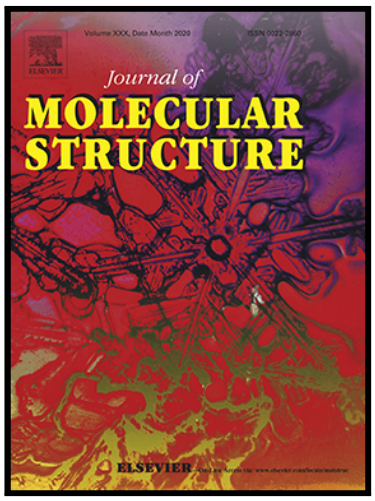

Synthesis, Characterization, in vitro and in silico studies of Bis-Hydrazone complexes derived from Terephthalic dihydrazide

Ramya Rajan M.P , Ramaswamy Rathikha , Rajendran Nithyabalaji , Rajendran Sribalan

PII: S0022-2860(21)00816-4
DOI: https://doi.org/10.1016/j.molstruc.2021.130683
Reference: MOLSTR 130683

To appear in: *Journal of Molecular Structure*

Received date: 28 December 2020
Revised date: 3 May 2021
Accepted date: 10 May 2021

Please cite this article as: Ramya Rajan M.P , Ramaswamy Rathikha , Rajendran Nithyabalaji , Rajendran Sribalan , Synthesis, Characterization, in vitro and in silico studies of Bis-Hydrazone complexes derived from Terephthalic dihydrazide, *Journal of Molecular Structure* (2021), doi: https://doi.org/10.1016/j.molstruc.2021.130683

Highlights

- The synthesized BHCs showed very good antidiabetic activity.
- The BHB showed 5 hydrogen bonding interaction with α-amylase.
- The BHS showed 5 hydrogen bonding interaction with α-glucosidase.
- The BHA showed highest α-amylase inhibition than others.
- The BHS showed highest α-glucosidase inhibition than others.

Synthesis, Characterization, *in vitro* and *in silico* studies of Bis-Hydrazone complexes derived from Terephthalic dihydrazide

Ramya Rajan M.P,[a,b *] Ramaswamy Rathikha,[b] Rajendran Nithyabalaji,[a] Rajendran Sribalan[c]

[a]*Department of Physics, SRM Valliammai Engineering College, Kattankulathur, Chengalpet Dt., Tamil Nadu, India*

[b]*PG & Research Department of Physics, Presidency College, Chennai, Tamil Nadu, India*

[c]*Biochemie Innovations Lab, Tindivanam, Tamil Nadu, India.*

Corresponding author e-mail:* ***ramyarajanmp@gmail.com*

Abstract

Bis-hydrazone of terephthalic dihydrazide was designed and synthesized using terephthalic dihydrazide and picolinaldehyde. Various bioactive benzoic acids such as benzoic acid, aspirin and salicylic acid were selected as a counter ion moiety for preparing bis-hydrazone complexes (BHCs). The prepared BHCs were well characterized using spectroscopic techniques like ^{1}H NMR, ^{13}C NMR and FT-IR. The BHCs showed very good *in vitro* antidiabetic activity in the α-amylase enzyme inhibitory method and moderate activity in the α-glucosidase inhibitory method. The molecular docking interactions of BHCs were performed against the human pancreatic α-amylase enzyme (1HNY.pdb) and homology model of α-glucosidase (3A4A.pdb) to prove the enzyme inhibitory activity. The BHCs showed very good binding energy, the complexes BHB showed 5 numbers of hydrogen bonding interactions with amino acid residues of 1HNY.pdb and BHS showed 5 numbers of hydrogen bonding interactions with 3A4A.pdb. Further, the molecular orbital studies were performed using density functional theory calculations in order to support the docking study.

Keywords: Bis-hydrazone; terephthalic dihydrazide; α-amylase inhibition; Molecular docking; DFT calculations.

1. Introduction

Type 2 diabetes mellitus is categorized by higher glucose levels in the blood and can lead to severe problems such as neuropathy, nephropathy, retinopathy and heart diseases[1,2]. The inhibition of carbohydrate digestion to the glucose unit is one of the significant therapeutic approaches for controlling the glucose level in the blood. The carbohydrate is hydrolyzed to glucose by hydrolyzing enzymes. α-amylase and α-glucosidases are the important enzymes for the hydrolysis of carbohydrates. The carbohydrates break down to small reducing sugars catalyzed by α-amylase and α-glucosidase and produce the small glucose unit [3,4]. Hence, to control hyperglycemia, the inhibition of α-amylase and α-glucosidase is an important therapeutic approach.

The therapeutic efficiency of combined drugs is more effective than a single agent [5]. In recent years, the combination therapy using dual/multiple drugs is a hopeful strategy for curing complex diseases [6]. The combinations of drugs have improved drug quality and improved therapeutic efficiency. For instance, both metformin and glyburide are used to treat type 2 diabetes patients. The insulin resistance is reduced by glyburide and insulin secretion is increased by metformin. In the combination of two or more drugs, the therapeutic efficacy improves by the complementary mechanism [7-8]. The physical and chemical properties of parent drugs are completely altered in the complexes. This process is a significant process in pharmaceutical research because the complexation enhances the stability and solubility of the lead compounds [9]. For example, the complex of theophylline with ethylenediamine (aminophylline) showed very good stability [10]. Similarly, the complexation of bioactive compounds with cyclodextrin was used to enhance the stability of the molecules [11].

The complexation of oppositely charged bioactive compounds has dual applications. It can act as a new drug complex and can act as new ionic complexes. Thus, the selection of

oppositely charged bioactive compounds for the synthesis of complexes may exhibit promising biological activities.

Hydrazones are simple derivatives of hydrazines. Moreover, hydrazones possess a wide range of pharmacological activities [12-13] and also hydrazones reduce the toxicity of hydrazines[14]. The metal complexes of hydrazone derivatives showed potent biological activities [15], the Schiff's base unit present in hydrazone is well-known bioactive moiety [16-20]. Several hydrazone derivatives are reported as potent bioactive compounds. Very few reports are available for bis-hydrazone's biological evaluations [21]. In this research, the bis-hydrazone has been selected as one of the bioactive compounds for complexation.

Similarly, benzoic acid is a well-known bioactive moiety and several benzoic acid derivatives are reported as bioactive compounds[22]. Benzoic acid, aspirin and nicotinic acid are some of the existing drugs available in the market. Based on the above ideas, in the present research, bis-terephthalic dihydrazone with various benzoic acid complexes (BHCs) was planned to synthesize for studying the α-amylase and α-glucosidase inhibition (Fig.1). Benzoic acid, aspirin and salicylic acid are selected as bioactive moieties for the complexation bis-hydrazone. The interaction of the α-amylase and α-glucosidase by BHCs was studied using molecular docking studies. On continuation, DFT calculations were performed in order to support the molecular docking interactions.

2. Experimental section

2.1. Materials and methods

The analytical grade solvents were used and purchased from Spectrochem or Sigma Aldrich. Reactions were monitored by the TLC plate which is on precoated silica gel 60 F_{254} in TLC sheets (0.2mm thickness, Merck plate) and 60-120 mesh Merck silica gel used for column

chromatography. Petroleum ether and ethyl acetate were used as the eluents. ^{1}H and ^{13}C NMR spectra were recorded on Bruker 500 MHz and 125 MHz instruments, $CDCl_3$ and DMSO-d_6 were used as an internal solvent. Chemical shift values were represented in δ (ppm) and coupling constants are mentioned in terms of Hz with the internal reference TMS. ESI-MS spectra were recorded in the LCQ fleet mass spectrometer. FT-IR spectra were recorded in Thermo Scientific Nicolet iS50 FT-IR Spectrometer.

2.2 Synthetic procedure for *N*'1,*N*'4-bis((*E*)-pyridin-2-ylmethylene)terephthalohydrazide (3)

The diethyl terephthalate (2g, 9.0 mmol) was dissolved in ethanol and hydrazine hydrate(80% in water) (1.12 mL, 18.0 mmol) was added at room temperature. The mixture was allowed to reflux for three hours. The completion of the reaction was monitored by thin layer chromatography. After completion of the reaction, the reaction mixture was allowed to room temperature and the reaction mixture was acidified with acetic acid. Then picolinaldehyde (1.712 mL, 18.0 mmol) was added and again refluxed for 3 hours. The completion of the reaction was monitored by thin layer chromatography. After completion of the reaction, the mixture was allowed to room temperature and poured into crushed ice. The obtained white precipitate was filtered and dried in a vaccum.[23]

White solid. Yield 88.2%. M.p. 255-257 °C. ^{1}H NMR (500 MHz, DMSO-d_6) δ 12.30 (s, 2H), 8.70 (d, J = 4.4 Hz, 2H), 8.56 (s, 2H), 8.15 (brs, 4H), 8.08 (d, J = 7.6 Hz, 2H), 7.98 (d, J = 7.6 Hz, 2H), 7.57 – 7.45 (m, 1H). ^{13}C NMR (125 MHz, DMSO-d_6) δ 163.1, 153.6, 150.0, 149.1, 137.3, 136.5, 128.4, 124.9, 120.5. ESI-MS calculated 372.13 found 373.10 $[M+1]^{+}$. IR (KBr Disc) cm^{-1}: 3412, 3301, 3053, 1647, 1582, 1284, 1147, 779, 713.

2.3. **Preparation of BHCs**

The Intermediate **3** (5 mmol) and corresponding carboxylic acid (5 mmol) were dissolved in ethanol (15 mL) and heated for 15 min and cooled to room temperature. The evaporation of the solvent yielded target compounds.

2.3.1 **2-((*E*)-(2-(4-(2-((*E*)-pyridin-2-ylmethylene)hydrazine-1-carbonyl)benzoyl)hydrazono)methyl)pyridin-1-ium benzoate (BHB)**

White solid. Yield 95.3 %. M.p. 249-251 °C. M.p. ^{1}H NMR (500 MHz, DMSO-d_6) δ 12.29 (s, 2H), 8.69 (d, *J* = 3.6 Hz, 2H), 8.57 (s, 2H), 8.14 (brs, 4H), 8.08 (d, *J* = 7.6 Hz, 2H), 8.00 (d, *J* = 7.6 Hz, 2H), 7.96 (d, *J* = 78.0 Hz, 2H), 7.66 (t, *J* = 7.3 Hz, 1H), 7.55 (t, *J* = 7.6 Hz, 2H), 7.52 – 7.47 (m, 2H). ^{13}C NMR (125 MHz, DMSO-d_6) δ 168.1, 163.3, 153.7, 150.1, 149.1, 137.5, 136.6, 133.2, 131.7, 129.8, 129.0, 128.5, 125.1, 120.6. IR (KBr Disc) cm^{-1}: 3414, 3197, 3031, 2866, 1756, 1643, 1573, 1298, 1189, 1144, 773, 706. Anal. Calculated for : $C_{27}H_{22}N_6O_4$; C, 65.58; H, 4.48; N, 16.99 %. Found; C, 65.54; N, 17.01; H, 4.47 %.

2.3.2. **2-((*E*)-(2-(4-(2-((*E*)-pyridin-2-ylmethylene)hydrazine-1-carbonyl)benzoyl)hydrazono)methyl)pyridin-1-ium 2-acetoxybenzoate (BHA)**

White solid. Yield 94.2%. M.p. 205-207 °C. ^{1}H NMR (500 MHz, DMSO-d_6) δ 12.28 (s, 2H), 8.69 (brs, 2H), 8.58 (s, 2H), 8.16 (brs, 4H), 8.07 (d, *J* = 7.1 Hz, 2H), 8.02 – 7.93 (m, 3H), 7.69 (t, *J* = 6.9 Hz, 1H), 7.50 (brs, 2H), 7.43 (t, *J* = 7.0 Hz, 1H), 7.25 (d, *J* = 7.7 Hz, 1H), 2.30 (s, 3H). ^{13}C NMR (125 MHz, DMSO-d_6) δ 169.7, 166.1, 163.1, 153.7, 150.7, 150.1, 149.1, 137.4, 136.5, 134.3, 131.9, 128.4, 126.6, 125.0, 124.6, 124.3, 120.5, 21.3. IR (KBr Disc) cm^{-1}: 3413, 3199, 3032, 2863, 1645, 1572, 1294, 1243, 1144, 769, 705. Anal. Calculated for: $C_{29}H_{24}N_6O_6$; C, 63.04; H, 4.38; N, 15.21 %. Found; C, 63.05; N, 15.18; H, 4.39 %.

2.3.3. **2-((*E*)-(2-(4-(2-((*E*)-pyridin-2-ylmethylene)hydrazine-1-carbonyl)benzoyl)hydrazono)methyl)pyridin-1-ium 2-hydroxybenzoate hydrate (BHS)**

White solid. Yield 93.9%. M.p. 208-210 °C. ^{1}H NMR (500 MHz, DMSO-d_6) δ 12.28 (s, 2H), 8.70 (brs, 2H), 8.58 (s, 2H), 8.16 (brs, 4H), 8.07 (d, *J* = 7.3 Hz, 2H), 7.97 (d, *J* = 6.8 Hz, 2H), 7.84 (d, *J* = 7.0 Hz, 1H), 7.56 (d, *J* = 7.0 Hz, 1H), 7.50 (brs, 2H), 7.05 – 6.96 (m, 2H). ^{13}C NMR (125 MHz, DMSO-d_6) δ 172.4, 163.1, 161.7, 153.7, 150.1, 149.1, 137.4, 136.5, 135.9, 130.8, 128.4, 125.0, 120.5, 119.5, 117.5, 113.8. IR (KBr Disc) cm^{-1}: 3412, 3196, 3028, 2863, 1642, 1572, 1290, 1143, 775, 706. Anal. Calculated for: $C_{27}H_{22}N_6O_5$; C, 63.52; H, 4.34; N, 16.46 %. Found; C, 63.56; N, 16.45; H, 4.33 %.

2.4 Antidiabetic Activity

2.4.1 *α*-amylase inhibitory activity

The antidiabetic activity was performed using the α-amylase inhibitory method as per reported literature with minor modification [24]. The detailed procedure was given in supporting information

2.4.2. α-glucosidase inhibitory activity

The antidiabetic activity was performed using the α-glucosidase inhibitory method as per reported literature [25].

2.5 Molecular docking study

The molecular docking interactions of BHCs were performed followed by Kathiresan *et a*l [26]. Molecular docking studies of BHCs were carried out with crystal structures of IHNY & 3A4A and performed using the Hex 8.0 software. The 3D structure of BHCs was constructed

using ChemBio 3D ultra 13.0 software and then they were energetically minimized using MMFF94 with the maximum number of iteration of 5000 and a minimum RMS gradient of 0.10 [27]. The crystal structure of the 1HNY & 3A4A was taken from Protein Data bank (www.rcsb.org) and all bound water and ligand were eliminated from the enzyme before docking. The docking parameters were used as default in Hex 8.0.

2.6 Computational calculations

All the computational calculations including representation of HOMO and LUMO in the checkpoint files were performed with the Gaussian 09W program using the DFT method [28]. The chemical structure of the BHCs was optimized with the B3LYP/6-31G basis set. The Gauss view software package was used to visualize the computed structures including HOMO, LUMO and Molecular electrostatic potential (MEP) representations.

3. Results and Discussions

3.1. Chemistry

The designed BHCs were synthesized from the commercially available diethylterephthalate. The reaction of diethylterephthalate with hydrazine hydrate gives the terephthalohydrazide (2). The Intermediate 2 was taken to the next step without isolation. The major Intermediate 3 was prepared from Intermediate 2 *via* the *in situ* manner using 2-pyridinecarbaldehyde by regular Schiff base synthesis. The acetic acid was used as a catalyst and ethanol is used as a solvent for the synthesis of Schiff base. The final complexes were prepared from Intermediate 3 with the reaction of aromatic carboxylic acids like benzoic acid, aspirin and salicylic acid. The outline for the synthesis of BHCs was represented in Scheme 1.

3.1.1. **Characterization**

The Intermediate 3 and BHCs were characterized by ^{1}H NMR, ^{13}C NMR and FT-IR spectroscopies. The Intermediate 3 was additionally characterized by ESI-Mass spectroscopy. The selected ^{1}H NMR and ^{13}C NMR chemical shifts are represented in Fig. 2.

3.1.1.1. Bis-hydrazone-benzoic acid complex (BHB)

The total number of protons in BHB was calculated to be 22 includes the pyridinium proton. The ^{1}H NMR spectrum very clearly showed that the integrated spectrum contains 21 numbers of protons (The pyridinium quarternary proton is a labile proton it may not appear in the spectrum). Similarly, the BHB contains 10 sets of protons excludes the pyridinium proton, the peaks appeared for 10 sets of protons. The singlet that appeared at 12.29 ppm indicates the presence of a hydrazone NH unit. The appearance of singlet at 8.57 ppm for 2 protons indicates the presence of imine CH unit which confirms the formation of hydrazone derivative. The doublet at 8.69 ppm for 2 protons has appeared for 2a & 25a protons of BHB. The appearance of peaks at 8.08, 7.96 and 7.55 ppm indicates the presence of a pyridine unit. The broad peak at 8.16 ppm for 4 protons appeared which is belongs to the phenylene unit of bis-hydrazone. The appearance of the triplet at 7.66 ppm has appeared for 30a proton. Similarly, the peaks at 7.52-7.47 & 8.00 ppm appeared for 29a & 31a, 28a & 32a protons respectively. It confirms the presence of the benzoate unit.

In ^{13}C NMR, the total number of carbon signal count was calculated to be 14. The BHB contains 14 sets of carbon. The appearance of the carbon signal at 168.1 ppm showed that the presence of carboxylate carbon which is present in the benzoate unit. The hydrazone carbonyl signal has appeared at 163.3 ppm. The peaks at 153.7 and 150.1 ppm have appeared for 6a &

21a, 2a & 25a carbon respectively which confirms the presence of the pyridine unit. The imine carbon signal has appeared at 149.1 ppm. The phenylene CH carbon signals have appeared at 128.5 ppm respectively. The peaks at 129.8, 129.0 and 133.2 ppm appeared for ortho, meta and para carbons of benzoate moiety correspondingly.

The FT-IR spectrum gave some additional information for the formation of BHB. The aromatic CH stretching frequencies absorbance was identified at 3196 and 3028 cm^{-1} respectively. The absorbance at 3412 cm^{-1} was identified which is appeared due to the presence of NH moiety which is present in hydrazone. The absorbance at 1756 cm^{-1} appeared due to the presence of a carboxylate unit which is present in benzoate moiety. The stretching frequency at 1643 $cm^{-1}$was appeared for the carbonyl unit present in the hydrazone moiety. The absorbance at 1573 cm^{-1} indicates the presence of an imine unit. The absorbance at 1298 cm^{-1} indicates the presence of C-N stretching vibrations.

3.1.1.2. Bis-hydrazone-aspirin complex (BHA)

The total number of protons in BHA is calculated to be 24 includes pyridinium proton. The ^{1}H NMR showed that the signals for 23 protons (pyridinium proton is labile proton which may not appear). The singlet at 12.28 ppm appeared for NH of the hydrazone unit and the singlet appeared at 8.58 ppm appeared for the imine CH unit. The proton signal at 8.69 ppm has appeared for 2b & 25b protons which are attached in the pyridine unit. The remaining pyridine protons have appeared at 7.05, 8.02-7.93 and 8.07 ppm respectively. The phenylene CH protons have appeared at 8.16 ppm as the broad signal. The aspirin unit contains 4 different environmental aryl protons which have different chemical shift values. The aryl protons of

aspirin appeared at 8.06-7.96, 7.69, 7.43 and 7.25 ppm correspondingly. The appearance of singlet at 2.30 ppm indicates the presence of acetyl CH_3 which is present in the aspirin unit.

The ^{13}C NMR showed 18 numbers of signals for BHA, the BHA contains 18 sets of carbons. The signals at 169.7, 166.1 and 163.1 ppm indicate the presence of carboxylate, ester and hydrazone carbonyl units. The carbon signal at 150.1 ppm appeared for 2b & 25b carbons respectively. The peak at 149.1 ppm appeared for the imine CH unit which is present in hydrazone moiety. The phenylene CH unit has appeared at 128.44 ppm respectively. The acetate CH_3 carbon of aspirin has appeared at 21.3 ppm, the peaks at 126.6, 131.8 and 134.3 ppm have appeared for aryl carbons of the aspirin unit. In addition, the FT-IR spectrum gave some additional information for the BHA formation. The absorbance at 3413 cm^{-1} indicates the presence of NH unit. The aromatic CH stretching frequencies have appeared at 3199 and 3032 cm^{-1} respectively. The absorbance at 1645 cm^{-1} indicates the presence of C=O stretching frequency and absorbance at 1572 cm^{-1} indicates the presence of C=N stretching frequency. The absorbance at 1294 cm^{-1} indicates the presence of C-N stretching vibrations.

3.1.1.3 Bis-hydrazone-salicylic acid complex (BHS)

The BHS contains 24 numbers of protons includes phenolic hydroxyl and pyridinium proton. The ^{1}H NMR clearly showed signals for 20 protons (phenolic hydroxyl and pyridinium protons are labile protons which may not appear). The singlet at 12.28 ppm appeared for the NH of hydrazone and the singlet at 8.58 ppm appeared for imine CH of the hydrazone unit. The signal appeared at 8.69, 8.07, 7.97 and 7.05 ppm indicates the presence of a pyridine unit. The phenyl CH protons have appeared at 8.16 ppm respectively. Similarly, the appearance of signals at 7.05-6.96, 7.56 and 7.84 ppm indicate the presence of a salicylate unit.

The BHS contains 16 sets of carbon, the ^{13}C NMR clearly displayed the 16 carbon signals. The carbon signal at 172.4 ppm appeared for carboxylate carbon which is present in the salicylate unit. Similarly, the signal at 163.1 ppm appeared for the hydrazone carbonyl unit. The carbon signal at 149.1 ppm appeared for the imine CH unit which is present in the hydrazone moiety. The carbon signal at 150.1 ppm appeared for 2c & 25c carbons and the phenylene CH carbon appeared at 128.45 ppm respectively. The carbon signal at 161.7 ppm appeared for 28c carbon which is present in the salicylate unit. The FT-IR spectrum gave some additional information for the formation of BHS. The absorbance at 3412 cm^{-1} appeared for NH stretching frequency. The aromatic CH stretching vibrations have appeared at 3196, 3028 cm^{-1} respectively. The absorbance at 1642 cm^{-1} indicates the presence of C=O stretching vibration and absorbance at 1572 cm^{-1} indicates the presence of C=N stretching vibrations. The absorbance at 1290 cm^{-1} indicates the presence of C-N stretching vibrations.

3.2 Biological evaluation

3.2.1 antidiabetic activity

3.2.1.2 α-amylase inhibitory method

The α-amylase enzyme present in the pancreas plays a crucial role in starch/carbohydrates digestion which breaks down the carbohydrates/starch to small reducing sugars. The inhibition of α-amylase leads to the reduction of postprandial hyperglycemia in diabetic conditions. The BHCs were tested for their antidiabetic activity using α-amylase enzyme by the DNSA method followed by Al-Zuhair *et al and* Kavitha *et al* with minor modification [24,29]. The α-amylase inhibition was performed in concentration dependent manner, the concentration of enzyme and substrate is fixed and starch has been used as a substrate. The % inhibitions against α-amylase enzyme were tested at various concentrations (10,

25, 50, 100 and 200 µg/mL) of BHCs and acarbose was used as a reference drug. The BHCs showed very good α-amylase inhibitory activity and their % inhibitions are nearer to standard acarbose. The increasing concentration showed increasing percentage inhibition of the enzyme. Amid three BHCs, BHB showed the highest inhibition than others. Comparatively, the α-amylase inhibitory activity of BHCs was in the order of BHB>BHS>BHA respectively. The % inhibitions at various concentrations were represented in Fig 3. On continuation, 50% inhibitory concentrations (IC_{50}) were also calculated for the α-amylase inhibition and the IC_{50} of BHB, BHA, BHS and Acarbose are calculated to be 101.11±3.51, 80.77±2.03, 91.64±2.21 and 66.32±1.84µg/mL respectively.

3.2.1.3 α-glucosidase inhibitory method

The α-glucosidase plays a similar role as α-amylase which converts the starch/polysaccharides to small glucose unit. . The inhibition of α-glucosidase also leads to the reduction of postprandial hyperglycemia in diabetic conditions Thus, the BHCs were tested for their antidiabetic activity using α-glucosidase enzyme followed by literature report [25]. The α-glucosidase inhibition was also studied by concentration dependent manner. The %inhibitions against α-glucosidase enzyme were tested at various concentrations (10, 25, 500, 100 and 200 µg/mL) of BHCs and acarbose was used as a reference drug. The increasing concentration of BHCs and standard showed increasing percentage inhibition of the enzyme. The BHCs showed very moderate α-glucosidase inhibition and their % inhibitions are moderate to reference. Amid three BHCs, BHS showed the highest inhibition than others. Comparatively, the α-glucosidase inhibition of BHCs was in the order of BHS>BHB>BHA respectively. The % inhibitions at various concentrations were represented in Fig 4. On continuation, 50% inhibitory concentrations (IC_{50}) were also calculated α-glucosidase inhibition and the IC_{50} of BHB, BHA,

BHS and Acarbose are calculated to be 120.62±1.65, 131.43±1.14, 113.06±1.01 and 72.34±1.51µg/mL respectively.

3.3 Computational studies.

3.3.1.1.Molecular docking studies for α-amylase inhibition.

Molecular docking is the significant computational tool which has been using to design the structure-based drug, predict the interaction of ligand to the applicable binding site of the enzyme and to develop the new bioactive compound [30]. α-amylase present in the pancreas and α-glucosidase present in the intestine is a crucial enzyme catalyzes the hydrolysis of starch/carbohydrates. The α-amylase inhibitors possess a vital role in minimizing diabetic complications. Thus the research is planned to select the pancreatic α-amylase enzyme and homology model of α-glucosidase for the molecular docking studies [31].

All the BHCs showed excellent binding energy with a α-amylase enzyme. The hydrogen bonding interactions play an important role in enzyme inhibition. Amid three BHCs, BHB and BHS showed more hydrogen bonding interaction with amino acid residues of α-amylase. The BHB showed 5 numbers of hydrogen bonding interactions. The BHB showed the binding energy of -361.59 KJ/mol and it forms the hydrogen bonding with LYS227, SER3, ASN5, THR6 and ARG291. The oxygen of hydrazone forms hydrogen bonding interaction with NH of LYS227 and the bond distance is found to be 1.98Å. The oxygen of benzoate ketone forms hydrogen bonding interaction with THR6 and the bond distance is found to be 3.06Å. The same oxygen forms another hydrogen bonding interaction with ASN5 and the bond distance is found to be 2.36Å. Similarly, the same oxygen forms hydrogen bonding with OH of SER3 and bond distance was found to be 2.81Å respectively.

The binding energy of BHA was calculated to be -386.89 KJ/mol and the BHA forms hydrogen bonding interaction with amino acid residues like TRP269 and ARG319. The oxygen of hydrazone forms hydrogen bonding interaction with indole NH of TRP269 and the bond distance is found to be 1.77Å. The calculated binding energy of BHS was found to be -357.53 KJ/mol. The pyridyl CH forms the hydrogen bonding interaction with the oxygen of THR6 and the bond distance is found to be 2.42Å. THR6 has another hydrogen bonding interaction with the oxygen of carboxylate and the bond distance is found to be 2.79Å. The same carboxylate forms another hydrogen bonding interaction with NH of ASN5 and the bond distance is found to be 1.94Å. The hydroxyl oxygen forms hydrogen bonding interaction with carboxamide NH of GLN8 and the calculated bond distance is found to be 3.09Å. Along with hydrogen bonding interactions, some other interactions like pi-cation interaction, pi-alkyl interaction, pi-sigma interaction, unfavorable pump interactions and attractive charge interactions were also identified between BHCs and 1HNY. The binding energy and hydrogen bonded amino acid residues were represented in Table 1. The docking interactions of the BHCs-1HNY complex are represented in Fig 5.

3.3.1.2. Molecular docking studies for α-glucosidase inhibition.

The α-glucosidase present in the intestine is a significant enzyme that catalyzes the hydrolysis of starch/carbohydrates. The α-glucosidase inhibitors also possess a vital role in minimizing diabetic complications. Thus the research is planned to select the homology model of α-glucosidase enzymes for the molecular docking studies as followed by Rahim *et al* [32].

The BHCs showed very good binding energies with enzyme and their binding energies are better than α-amylase inhibition. And also, the hydrogen bonding interactions are similar to α-amylase enzyme inhibition. The BHB showed two hydrogen bonding with the binding energy of

-371.29 KJ/mol. The BHB forms the hydrogen bonding interaction with the amino acid residues of HIS280 and ASP325 and hydrogen bonding distances are found to be 2.75 and 1.65Å respectively. The binding energy of BHA is found to be -411.47 KJ/mol and it showed the highest binding energy than others. The BHA forms three hydrogen bonding interactions with the amino acid residues of HIS423, GLU422 and ARG315 and the hydrogen bonding distance was found to be 2.60, 2.95 and 2.90Å correspondingly. Similarly, the BHS showed five hydrogen bonding interactions with the amino acid residue of ASP352, GLN279, ARG315 and SER240. The BHS showed two hydrogen bonding interactions with ARG315. The hydrogen bonding distance with ASP352, GLN279, ARG315 and SER240 was found to be 1.61Å, 2.84, 2.69 & 3.18 and 2.38Å correspondingly. The binding energy of BHS is found to be -383.54 KJ/mol. Among BHCs, the BHS showed the highest number of hydrogen bonding interactions. A similar result was obtained in *in vitro* α-glucosidase inhibition because BHS showed the highest inhibition than others. The binding energy and hydrogen bonded amino acid residues were represented in Table 2. The docking interactions of the BHCs-3A4A complex are represented in Fig 6.

3.3.2. Frontier molecular orbitals

The highest occupied molecular orbital (HOMO) and lowest unoccupied molecular orbital (LUMO) are used to predict the chemical properties, electrical properties, biological activity, reactivity and stability of the complexes [33-34]. The molecular orbitals play a crucial role in the calculation of the HOMO, LUMO, bandgap and other parameters. The electron densities in the molecule are ready to form the interaction with enzymes. In BHCs, the electrons are localized over benzoate moiety in HOMO. But in the case of LUMO, the electron density is shifted to hydrazone moiety. Thus these regions (benzoate to hydrazone) are responsible for

making interaction with the enzyme. The same results were obtained in the molecular docking studies. Most of the hydrogen bonding interactions were identified in the carboxylate and hydrazone moieties.

The negative energies of HOMO (-5.4219 to -5.5202 eV) and LUMO (-2.7258 to -2.9280 eV) indicate the BHCs are stable molecules. The bandgap values are used to predict the chemical reactivity and stability of the molecule. Comparatively, the calculated bandgaps of BHCs are similar to each other. The bandgap values of BHCs were in the range of 2.493 to 2.784 eV respectively. The electrophilicity index is the tendency to accept electrons from the environment. Especially, the higher value of electrophilicity index has a higher ability to accept electrons from enzymes. But in BHCs, electrophilicity index values similar to each other. Hence the BHCs showed more or less similar α-amylase enzyme inhibitory activity and binding energy in molecular docking studies. The calculated electrophilicity index values of BHCs in the range of 5.9496 to 6.9890. In addition, some other DFT parameters like chemical potential, global hardness and global softness are also calculated and presented in Table 3. The optimized structure, HOMO and LUMO images were represented in Fig 7.

3.3.1 Molecular electrostatic potential

The binding region of a ligand with the biomolecules can be predicted using molecular electrostatic potential. In molecular electrostatic potential, the most positive potential is represented in blue colour and the most negative potential is represented in red colour. These potentials are significant for understanding the binding region responsible for the biological interactions of the ligand [34]. Particularly, the ligand's negative potential region is important because which makes hydrogen bonding interaction with the enzyme. In BHCs, the negative potential was identified in the region of carboxylate oxygen, oxygen of hydrazone and nitrogen

of pyridine. Comparatively the carboxylate oxygen showed more negative potential than others. And also hydrazone oxygen has a moderate negative potential. These regions showed more hydrogen bonding interactions with the 1HNY enzyme. The pyridine nitrogen displayed very little negative potential, this nitrogen does not forms any hydrogen bonding interaction with α-amylase. And also the most positive potential was identified in NH of hydrazone moiety. This region also forms hydrogen bonding interaction with the enzyme. From the molecular electrostatic potential results, the research concludes that the molecular docking results are coherent with molecular electrostatic potential. The molecular electrostatic potential image was represented in Fig 8.

4. Conclusions

The BHCs were successfully synthesized and well characterized using the spectroscopic technique. As expected, the BHCs showed α-amylase as well as α-glucosidase inhibitions. The binding energies are also similar to each other and BHB showed 5 hydrogen bonding interactions with the amino acid residue of 1HNY. The BHS showed 5 numbers of hydrogen bonding interactions with the amino acid residue of 3A4A. The reactivity or stability of the BHCs was also similar which is confirmed by the bandgap results of molecular orbital studies. The molecular electrostatic potential results were coherent with molecular docking interactions.

Acknowledgment

The authors grateful to Biochemie Innovations Lab, Tindivanam-604001 for consultancy service during this research work.

Figures and captions

Fig 1: 2D structures of designed BHCs

Fig 2: Selected ^{1}H and ^{13}C NMR chemical shifts of BHCs.

Fig 3: α-amylase inhibition of BHCs.

Fig 4: α-glucosidase inhibition of BHCs.

Fig 5: Docking interactions BHCs with 1HNY.

Fig 6: Docking interactions BHCs with 3A4A.

Fig 7: Frontier molecular orbitals of BHC_S

Fig 8: Molecular electrostatic potential of BHCs.

Scheme 1: Synthetic route for BHCs.

Tables and captions

Table 1: Docking interaction of BHCs against 1HNY.

Table 2: Docking interaction of BHCs against 3A4A.

Table 3: DFT calculations of BHCs.

Declaration of interests

The authors declare that they have no known competing financial interests or personal relationships that could have appeared to influence the work reported in this paper.

References

1. R. Pecoits-Filho, H. Abensur, C.C.R. Betônico, A.D. Machado, E.B. Parente, M. Queiroz, J.E.N. Salles, S. Titan, S. Vencio, Interactions between kidney disease and diabetes: Dangerous liaisons, Diabetol. Metab. Syndr. 8 (2016) 50.
2. S. Canivell, R. Gomis, Diagnosis and classification of autoimmune diabetes mellitus. Autoimmun. Rev. 13 (2014) 403–407.
3. Y. Hara, M. Honda The inhibition of alpha amylase by tea polyphenols. Agric. Biol. Chem. 54 (1990) 1939–45

4. T. Matsui, T. Tanaka, S. Tamura, A. Toshima, K. Tamaya, Y. Miyata et al. Alpha-glucosidase inhibitory profile of catechins and theaflavins. J. Agric. Food Chem. 55 (2007) 99–105.
5. J. Lehar, A. S. Krueger, W. Avery, A. M. Heilbut, L. M. Johansen, Synergistic drug combinations tend to improve therapeutically relevant selectivity, Nat. Biotechnol. 27 (2009) 659–666.
6. T. Stanton, J. L. Reid, Fixed dose combination therapy in the treatment of hypertension. J Hum. Hypertens. 16 (2002) 75–78.
7. S. U. Bokhari, U. M. Gopal, W. C. Duckworth, Beneficial effects of a glyburide/metformin combination preparation in type 2 diabetes mellitus. Am. J. Med. Sci. 325 (2003) 66–69.
8. X. M. Zhao, M. Iskar, G. Zeller, M. Kuhn, V. van Noort, P. Bork, Prediction of Drug Combinations by Integrating Molecular and Pharmacological Data. PLoS Comput. Biol. 7 (2011) e1002323.
9. M. M. Amiji, T. J. Cook, W. Cary Mobley, Complexation and Protein Binding, Book Chapter, Applied Physical Pharmacy. 2e.
10. P. M. Soares, M. C. A. Patrocínio, A. S. Assreuy, R. C. L. Siqueira, N. M. Lima , M.O.V. Arrud , S. S. Escudeiro , K. M. de Carvalhoa, F. C. F. Sousa, G. S. BarrosVian, S. M. M. Vasconcelos, Aminophylline (a theophylline–ethylenediamine complex) blocks ethanol behavioral effects in mice, Behav. Pharmacol. 20 (2009) 297–302.
11. V. B. Chaudhary, J. K. Patel, Cyclodextrin inclusion complex to enhance solubility of poorly water soluble drugs: a review, Int. J. Pharm. Sci. Res. 4 (2013) 68-76.
12. Md. R. Ali, A. Marella, Md. T. Alam, R. Naz, M. Akhter, Md. Shaquiquzzaman, R. Saha, O. Tanwar, Md. M. Alam, J. Hooda, Review of biological activities of hydrazones, Indonesian. J. Pharm. 23 (2012) 193-202.
13. S. S. Bharadwaj, B. Poojay, S. M. Kumar, K. Byrappa, G. S. Nagananda, A. K. Chaitanya, K. Zaveri, N. S. Yarla, Y. Shiralgi, A. K. Kudva, B. L. Dhananjaya, Design, Synthesis and pharmacological studies of some new quinoline Schiff bases and 2,5-(disubstituted-[1,3,4])-oxadiazles, New J. Chem. 41 (2017) 8568-8585.

14. M. J. Hearn and M. H. Cynamon, Design and synthesis of antituberculars: preparation and evaluation against *Mycobacterium tuberculosis* of an isoniazid Schiff base, J. Antimicrobial Chemother. 53 (2004) 185–191.
15. A. El-Dissouky, O. Al-fulaij, M. K. Awad, S. Rizk, Synthesis, characterization and biological activity studies of copper (II)- metal (II)binuclear complexes of dipyridylglyoxal bis(2-hydroxybenzoyl hydrazone), J. Coord. Chem. 63 (2010) 330-345.
16. V. R. Avupati, R.P. Yejella, V. R. Perala, K. N. Killari, V. M. R. Papasani, P. Cheepurupalli, V. R. Gavalapu, B. Boddeda, Synthesis, characterization and in vitro biological evaluation of some novel 1,3,5-triazine-schiff base conjugates as potential antimycobacterial agents, Bioorg. Med. Chem. Lett. 23 (2013) 5968-5970.
17. I. Yahaya, M. Chemchem, B. Aydiner, N. Seferoglu, F. E. Tepe, L. Acik, N. A. Cerci, M. Turk, Z. Seferoglu, Novel fluorescent coumarin-thiophene-derived schiff bases: synthesis,effects of substituents, photophysical properties, dft calculations, and biological activities, Photchem. Photobiol. A. 368 (2019) 296-306.
18. Z-M. Wang, S-SXie, X-M Li, J-JWu, X-B. Wang, L-Y. Kong, Multifunctional 3-schiff base-4-hydroxycoumarin derivatives with monoamine oxidase inhibition, anti-β-amyloid aggregation, metal chelation, antioxidant and neuroprotection properties against alzheimer's disease, RSC Adv. 5 (2015) 70395-70409.
19. S. Tariq, F. Avecilla, G. P. Sharma, N. Mondal, A. Azam, Design, synthesis and biological evaluation of quinazolin-4(3H)-one Schiff base conjugates as potential antiamoebic agents. J. Saudi Chem. Soc. 22 (2018) 306-315.
20. J. Zhang, P. Cheng, Y. Ma, J. Liu, Z. Miao, D. Ren, C. Fan, M. Liang, L. Liu, An efficient nano CuO-catalyzed synthesis and biological evaluation of quinazolinone Schiff base derivatives and bis-2,3-dihydroquinazolin-4(1H)-ones as potent antibacterial agents against streptococcus lactis, Tetrahedron Lett. 57 (2016) 5271-5277.
21. H. S. V. Jois, B. Kalluraya, T. Vishwanath, Synthesis, spectroscopic properties and antioxidant activity of bis-hydrazones and Schiff's bases derived from terephthalic dihydrazide, J. Fluoresc. 25 (2015) 481-488.
22. B-E, Amborabe, P. Fleurat-Lessard, J-F. Chollet, G. Roblin, Antifungal effects of salicylic acid and other benzoic acid derivatives towards eutypa lata: structure-activity relationship, Plant Physiol. Biochem. 40 (2002) 1051-1060.

23. A. S. Murugan, E. R. A. Noelson, J. Annaraj, Solvent dependent colorimetric, ratiometric dual sensor for copper and fluoride ions: real sample analysis, cytotoxicity and computational studies, Inorg. Chim. Acta 450 (2016) 131-139.
24. S. Al-Zuhair, A. Dowaidar, H. Kamal, Inhibitory Effect of Dates-extract on a-amylase and b-glucosidase Enzymes Relevant to Non-insulin Dependent Diabetes Mellitus, J. Biochem. Technol. 2 (2010) 158 – 160.
25. A. Y-T. Deng, S-Y. Lin-Shiau, J-K. Lin, Pu-erh tea polysaccharides decrease blood sugar by inhibition of α-glucosidase activity in vitro and in mice. Food Func.6 (2015) 1539-46.
26. S. Kathiresan, T. Anand, S. Mugesh, J. Annaraj, Synthesis, spectral characterization and DNS bindings of tridentate N_2O donor schiff base metal(II) complexes, Photochem. Photobiol. B. 148 (2015) 290-301.
27. Y.Y. Xu, Y. Cao, H. Ma, H.Q. Li, G.Z. Ao, Design, synthesis and molecular docking of α,β-unsaturated cyclohexanone analogous of curcumin as potent EGFR inhibitors with antiproliferative activity, Bioorg. Med. Chem. 21 (2013) 388-394.
28. M.J. Frisch, G.W. Trucks, H.B. Schlegel, G.E. Scuseria, M.A. Robb, J.R. Cheeseman, J.A. Montgomery Jr., T. Vreven, K.N. Kudin, J.C. Burant, J.M. Millam, S.S. Iyengar, J. Tomasi, V. Barone, B. Mennucci, M. Cossi, G. Scalmani, N. Rega, G.A. Petersson, H. Nakatsuji, M. Hada, M. Ehara, K. Toyota, R. Fukuda, J. Hasegawa, M. Ishida, T. Nakajima, Y. Honda, O. Kitao, H. Nakai, M. Klene, X. Li, J.E. Knox, H.P. Hratchian, J.B. Cross, V. Bakken, C. Adamo, J. Jaramillo, R. Gomperts, R.E. Stratmann, O. Yazyev, A.J. Austin, R. Cammi, C. Pomelli, J.W. Ochterski, P.Y. Ayala, K. Morokuma, A. Voth, P. Salvador, J.J. Dannenberg, V.G. Zakrzewski, S. Dapprich, A.D. Daniels, M.C. Strain, O. Farkas, D.K. Malick, A.D. Rabuck, K. Raghavachari, J.B. Foresman, J.V. Ortiz, Q. Cui, A.G. Baboul, S. Clifford, J. Cioslowski, S.B.B. tefanov, G. Liu, A. Liashenko, P. Piskorz, I. Komaromi, R.L. Martin, D.J. Fox, T. Keith, M.A. AlLaham, C.Y. Peng, A. Nanayakkara, M. Challacombe, P.M.W. Gill, B. Johnson, W. Chen, M.W. Wong, C. Gonzalez, J.A. Pople, Gaussian 03, Revision C.02, Gaussian, Inc., Wallingford, CT, 2004.
29. R. Kavitha, S. Nirmala, R. Nithyabalaji, R. Sribalan, Biological evaluation, molecular docking and DFT studies of charge transfer complexes of quinaldic acid with heterocyclic carboxylic acid, J. Mol. Struct. 1504 (2020) 127508.

30. K.P. Safna Hussan, M. Shahin Thayyil, Vijisha K. Rajan, K. Muraleedharan, DFT studies on global parameters, antioxidant mechanism and molecular docking of amlodipine besylate, Comput. Biol. Chem. 80, 2019, 46-53.
31. G. Banuppriya, R. Sribalan, S. A. R. Fathima, V. Padmini, Synthesis of b-Ketoamide Curcumin Analogs for Anti-Diabetic and AGEs Inhibitory Activities, Chem. Biodivers. 15 (2018) 1800105.
32. B. F. Rahim, K. Zamam, M. Taha, H. Ullah, M. Ghufran, A. Wadood, W. Rehman, N. Uddin, S. A. A. Shah, M. Sajid, F. Nawaz, K. M. Khan, Synthesis, in vitro alpha-glucosidase inhibitory potential of benzimidazole bearing bis-Schiff bases and their molecular docking study, Bioorg. Chem. 94 (2020) 103394.
33. K. Sarojinidevi, P. Subramani, M. Jeeva, N. Sundaraganesan, M. S. Boobalan, G. V. Prabhu, Synthesis, molecular structure, quantum chemical analysis, spectroscopic and molecular docking studies of N-(Morpholinomethyl) succinimide using DFT method, J. Mol. Struct. 1175 (2018) 609-623.
34. P. Shafieyoon, E. Mehdipour, Y. S.Mary, Synthesis, characterization and Biological Investigation of glycine- based sulfonamide derivative and its complex: vibration assignment, HOMO–LUMO analysis, MEP and molecular docking, J. Mol. Struct. 1181, (2019) 244-252.

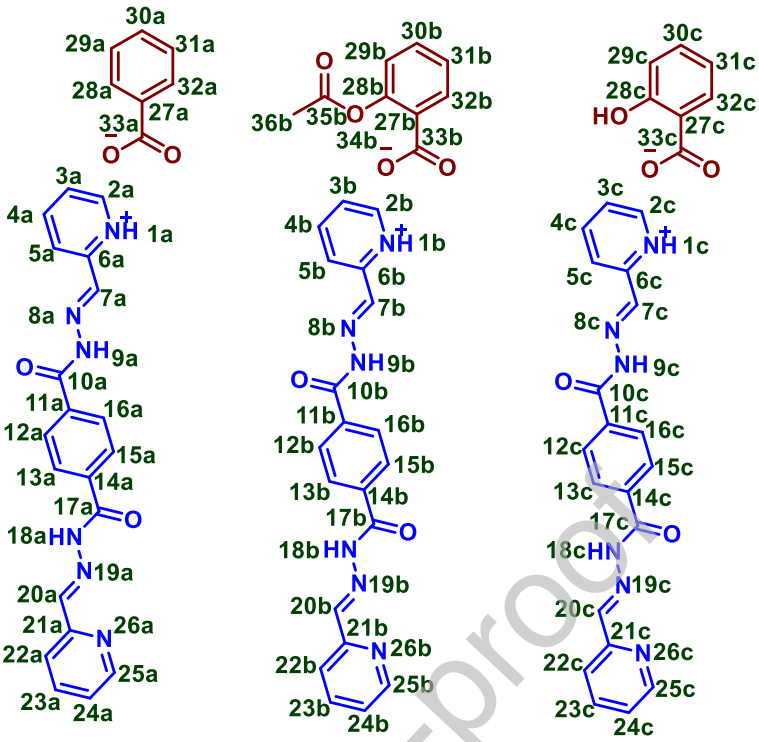

Fig 1: 2D structures of designed BHCs

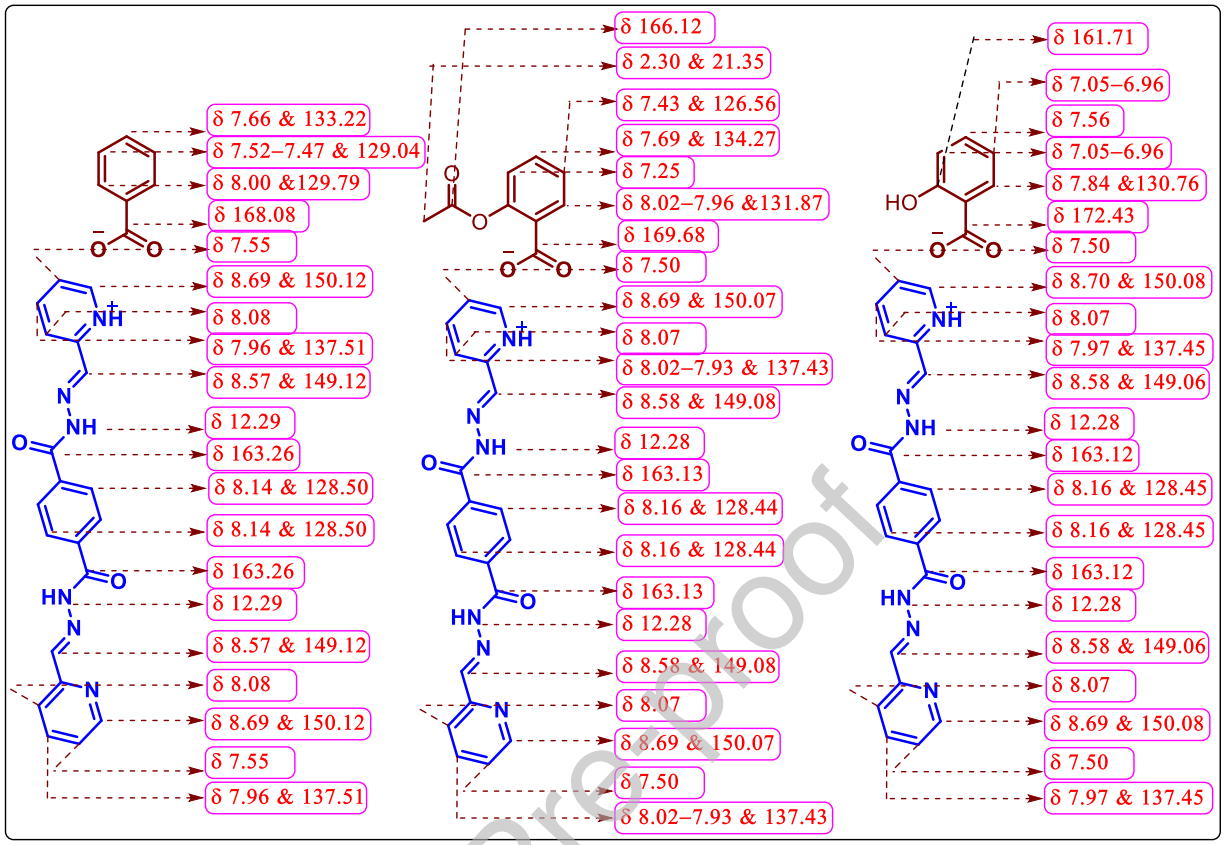

Fig 2: Selected ^{1}H and ^{13}C NMR chemical shifts of BHCs.

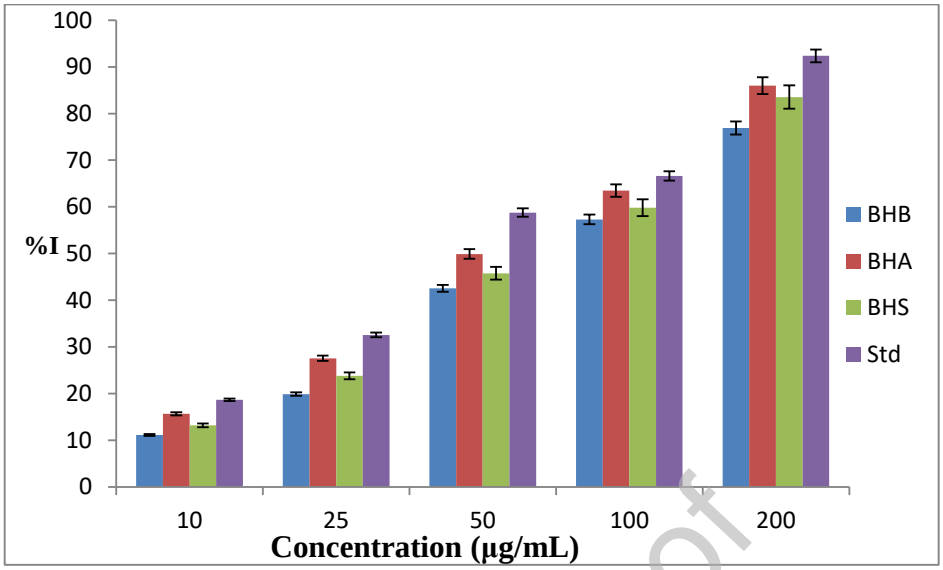

%I =% Inhibition

Fig 3: α-amylase inhibition of BHCs.

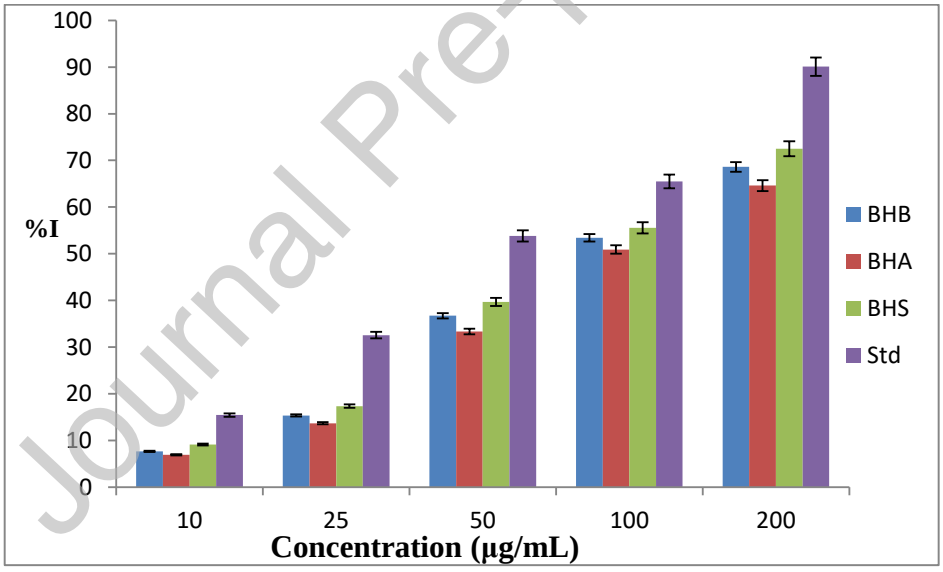

%I =% Inhibition

Fig. 4: α-glucosidase inhibition of BHCs

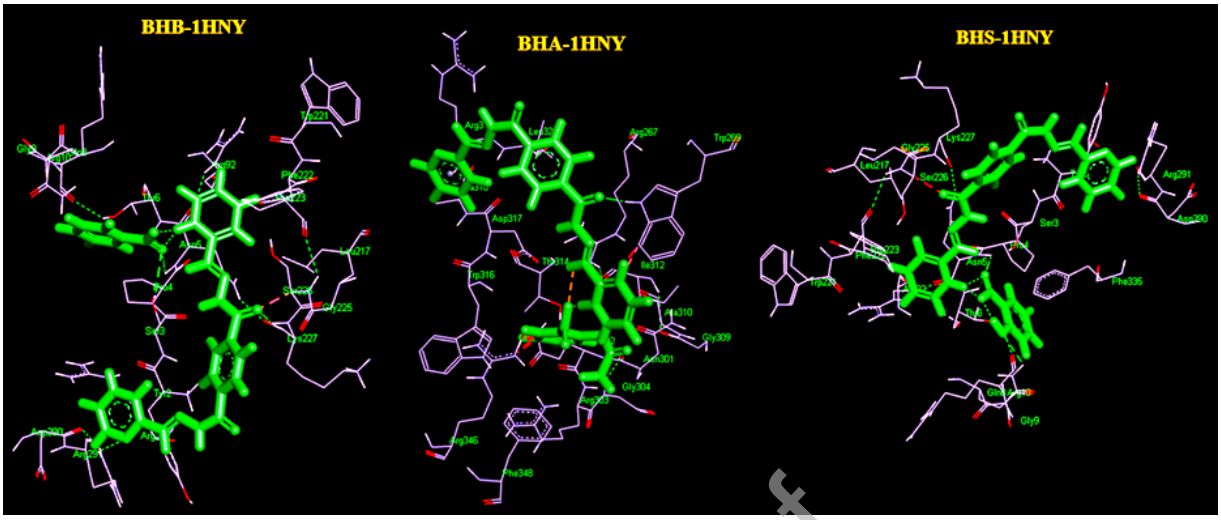

Fig 5: Docking interactions BHCs with 1HNY.

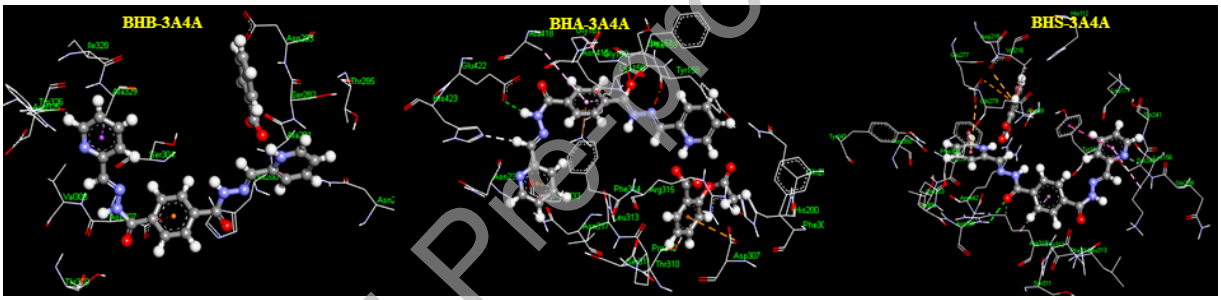

Fig. 6: Docking interactions BHCs with 3A4A.

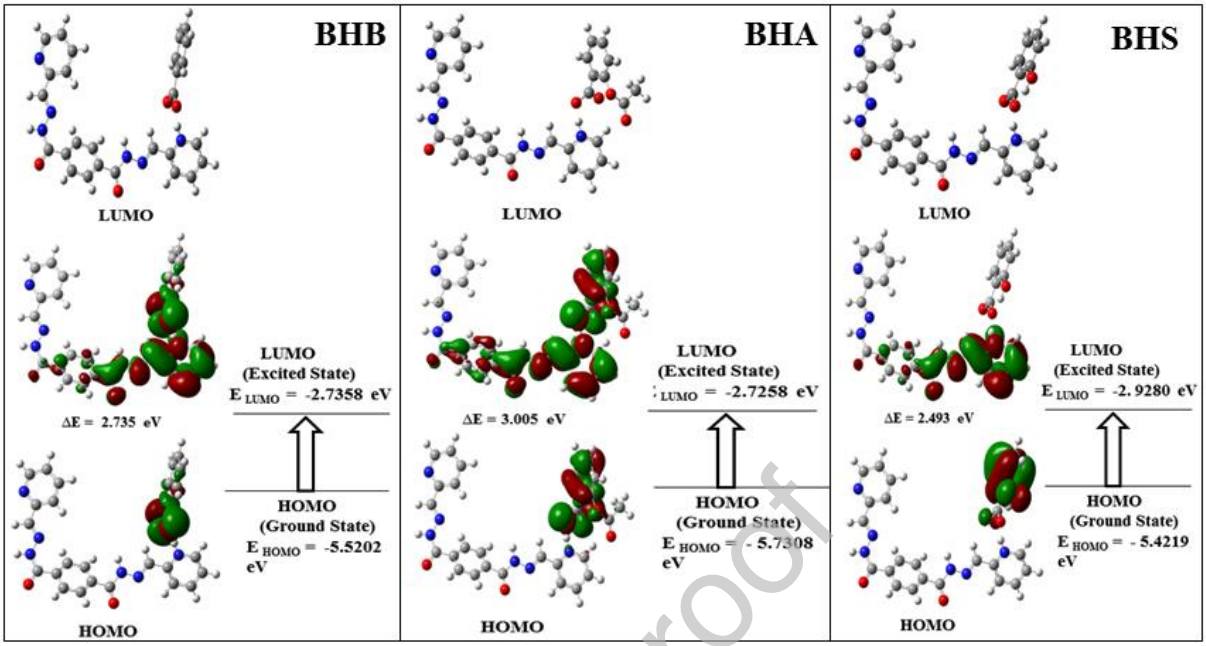

Fig 7: Frontier molecular orbitals of BHCs

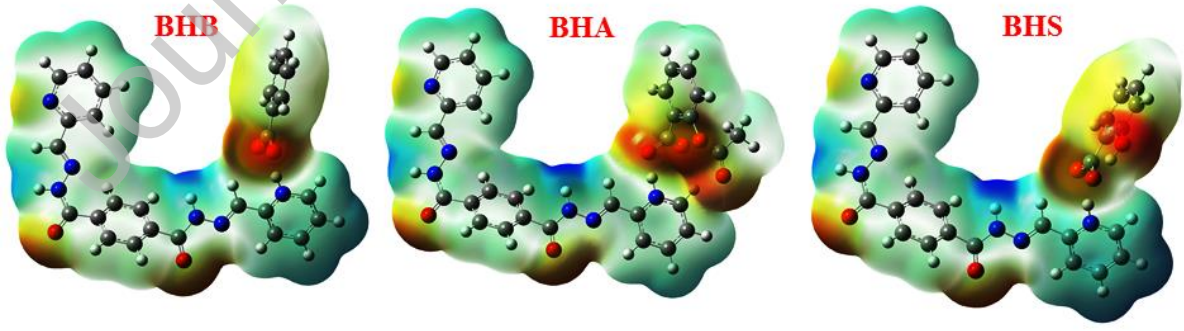

Fig 8: Molecular electrostatic potential of BHCs.

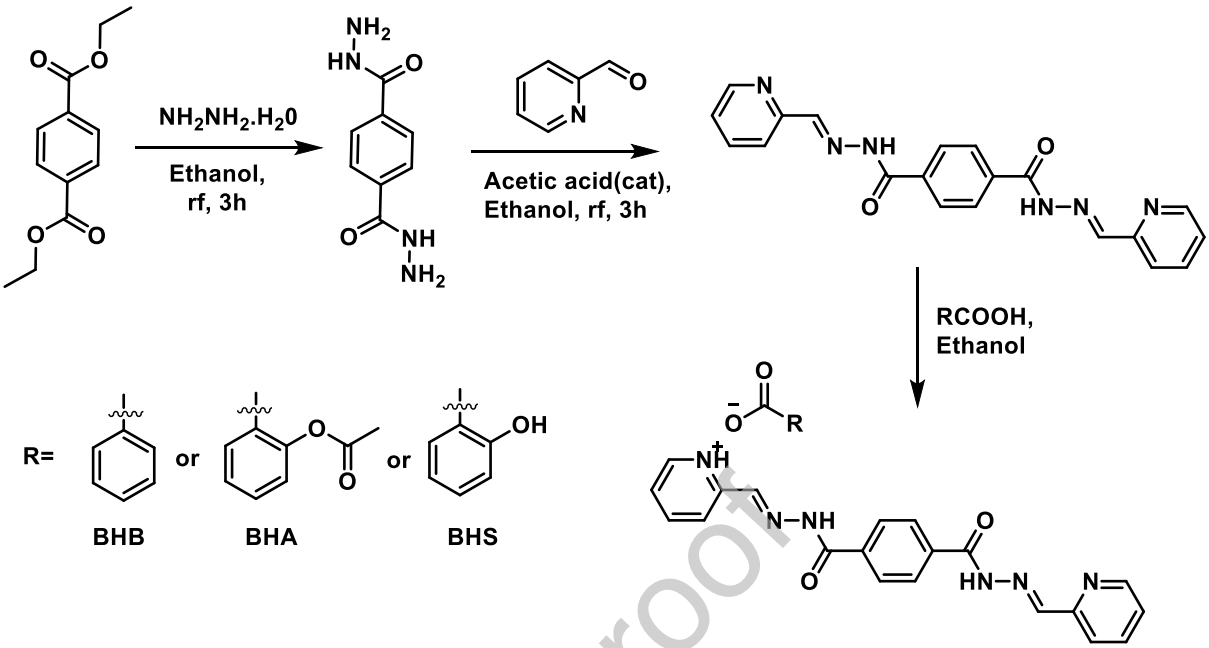

Scheme 1: Synthetic route for BHCs.

Table 1: Docking interaction of BHCs against 1HNY

S. No	Compound name	Binding energy KJ/mol	No. of hydrogen bonding	Interacted amino acid residue
1.	BHB	-361.59	5	LYS227,SER3,ASN5,THR6 ,ARG291
2.	BHA	-386.89	2	TRP269,ARG319
3.	BHS	-357.53	4	GLN8,ASN5,THR6(2)

Table 2: Docking interaction of BHCs against 3A4A

S. No	Compound name	Binding energy KJ/mol	No. of hydrogen bonding	Interacted amino acid residue
1.	BHB	-371.29	2	HIS280, ASP325
2.	BHA	-411.47	3	HIS423, GLU422, ARG315
3.	BHS	-383.54	4	ASP352, GLN279, ARG315(2), SER240

Table 3: DFT calculations of BHCs.

S. No	Compound name	HOMO	LUMO	Bandgap (ΔE)	Chemical potential	Global hardness	Global softness	Electrophillicity index
1.	BHB	-5.5202	-2.7358	2.784	-4.1280	1.3921	0.3591	6.1202
2	BHA	-5.7308	-2.7258	3.005	-4.2283	1.5025	0.3327	5.9496
3	BHS	-5.4219	-2.9280	2.493	-4.1750	1.2469	0.4009	6.9890

Graphical Abstract